EPSC Abstracts
Vol. 13, EPSC-DPS2019-456-2, 2019
EPSC-DPS Joint Meeting 2019

EPSC-DPS Joint Meeting 2019
15–20 September 2019 | Geneva, Switzerland

Geometric preprocessing for Rosetta/VIRTIS-M measurements of comet 67P/C-G

D. Kappel (1,2), G. Arnold (2), L.V. Moroz (2), A. Raponi (3), M. Ciarniello (3), F. Tosi (3), S. Erard (4), C. Leyrat (4), M. I. Błęcka (5), G. Filacchione (3), F. Capaccioni (3), and the Rosetta/VIRTIS Team
(1) Institute of Physics and Astronomy, Univ. of Potsdam, Germany, dakappel@uni-potsdam.de, (2) Institute of Planetary Research, DLR, Berlin, Germany, (3) INAF-IAPS, Rome, Italy, (4) LESIA, Observatoire de Paris, Université PSL, CNRS, Sorbonne Université, Univ. Paris Diderot, Sorbonne Paris Cité, France, (5) SRC PAS, Bartycka 18a, 00-716 Warsaw, Poland

Abstract

Following earlier surface spectrophotometric analyses [1] of Rosetta/VIRTIS-M measurements of comet 67P/Churyumov-Gerasimenko (hereafter 67P), we refine the instrument's geometric registration model and spatial consistency of the radiometric calibration. For this purpose we compare measured 67P nucleus images from the entire mission to corresponding photometric simulations and determine an optical distortion map between them. The refinements will allow us to improve the retrieval of physical and compositional surface properties of the comet's nucleus.

1. Introduction

The mapping channel (VIRTIS-M) of the VIRTIS instrument aboard ESA's Rosetta mission acquired spectrally resolved images of the nucleus surface of comet 67P (VIS: 0.22-1.05 µm, IR: 0.95-5.1 µm) [2]. At each exposure a frame of 432 spectral channels (or effective wavelengths) times 256 spatial pixels ('samples', IFOV 0.25 x 0.25 mrad^2) was recorded in the VIS or IR, respectively. By scanning the scene with a movable mirror at steps of 1 IFOV, series of these spectrally resolved lines were collected into so-called data cubes. There were 257 possible mirror angles ('absolute lines' from -128 to 128), but for most cubes only part of this range was used.

Comparing spectrophotometric measurements to corresponding simulations enables constraining physical and compositional properties of regolith surfaces. Here, the link between surface properties and radiance spectra can be provided by radiative transfer models like those of Hapke [3] or Shkuratov [4]. For a reliable simulation as needed for the retrieval of surface properties, such models require accurate information on illumination and observation geometry and thus a precise geometric match of measured VIRTIS-M images and simulated ones. However, detailed comparisons between the measured images and standard pipeline geometry simulations reveal locally varying spatial mismatches of up to a few pixels. It is challenging to precisely calibrate this complex instrument [5,6], and for instance due to mechanical and thermal stresses during the launch, cruise, and flyby phases of the mission, the ground calibration of the geometric distortion and the radiometric calibration may not accurately represent the state of the instrument during the measurements anymore. In the present work, we intend to improve the geometric match, and in the same step we can obtain a correction factor that improves the spatial consistency of the radiometric calibration.

2. Geometric modeling

An accurate spectrophotometric analysis of the VIRTIS-M measurements of the nucleus surface calls for precise geometry information, in particular for incidence, emergence, and phase angles at the intersection of the respective viewing rays from the instrument pixels with the nucleus surface, in addition to the shadowing state there. We compute these data using the SPICE toolkit [7] and the necessary navigational data bases (SPICE kernels) for the Rosetta mission as well as an accurate high-resolution digital shape model [8]. While the planned photometric modeling is intended to make use of, e.g., the Hapke model [3], the following purely geometric analysis is based on the parameterless Akimov disk function [4]. The latter one well describes the topography-dependent photometric behavior of an utterly rough surface and is computationally quite inexpensive. To capture the effect of shape model variations inside the single pixels' footprints and enable a flexible investigation of the VIRTIS-M instrumental point spread function (PSF) (location of peak, width, possible deviations from a Gaussian, all in dependence on sample, absolute line, and wavelength), we sample each pixel's field-of-view (FOV) including a certain margin by a dense grid of viewing rays. The footprints on the shape model and the necessary geometric data are computed using SPICE, and the Akimov disk function is applied for each ray and set to zero in case the footprint is in shadow. Now this proxy for the relative spatial variation of the surface signal is convolved with a simple model for the PSF (Gaussian peaking at the pixel center and with a full-width-at-half-maximum, FWHM, of one nominal pixel FOV). Significant deviations between the resulting synthetic VIRTIS-M image and the measurement show up.

3. Feature-based image matching

To obtain a first-order correction of this misalignment, we apply the feature-based local image matching algorithm GeFolki [9], which yields for each pixel a shift vector in sample and in line direction that leads to a much better geometric match. Due to the feature-rich character of the 67P topography and the high quality and resolution of the shape model, this shift vector field is quite well defined. In addition, we compute for each spatial line the ratio between the measured radiance and the geometrically matched simulated radiance proxy to avoid observation bias in the determination of the spatial radiometric correction factor below. This ratio is suitably normalized to carry just the information on possible inhomogeneities of the radiometric calibration depending on spatial sample. The entire approach is performed for all spectral channels and all VIS and IR cubes that sound the nucleus. Finally, the shift vectors are averaged over all cubes as functions of spectral channel, sample, and absolute line, and the inhomogeneity factors as functions of channel and sample. For stability reasons we take into account only cubes where a large portion of the FOV is filled with the nucleus' illuminated parts. In a subsequent step, these corrections are applied in the simulation, and the FWHM of the PSF and slight deviations from a Gaussian are retrieved in addition (Fig. 1).

4. Results

The dependence of the shift vectors on spectral channel, spatial sample, and mirror angle cannot be explained by misrepresentations of instrument position and pointing in the SPICE kernels, although these may contribute to the mismatch for individual cubes. Rather we interpret the behavior as a consequence of non-trivial variations of the PSF in terms of location of the peak and FWHM, in other words of optical distortions, possibly also in correlation with the instrument temperature.

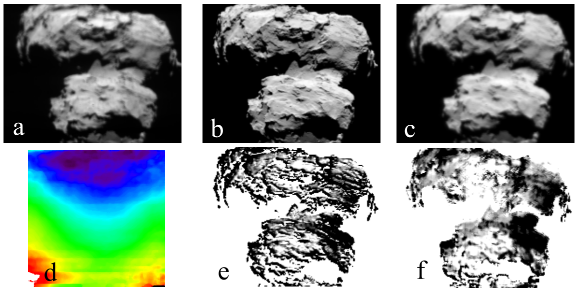

Figure 1: Comparison of measurement and simulations for VIRTIS-M-IR cube I1_00383489908. (a) radiance measurement at 1 µm; (b) simple simulation; (c) corrected simulation; (d) example for shift in line direction as function of sample (horizontal axis, between 1 and 256) and absolute line (vertical axis, between -128 and 128), blue=-1.5 px, white=+1.5 px; (e) ratio of a to b; (f) ratio of a to c. For e and f: black=0.9, white=1.1 on a relative scale.

The overall behavior of both the VIS and the IR shifts in the spatial directions are reminiscent of the smile and keystone optical distortions. Differences in the wavelength-dependencies of the shifts like they occur at the IR spectral order-sorting-filter transitions point to, e.g., effects from detector coatings. Except for the detector edges, the relative radiometric correction factor deviates from unity by the order of typically a few and up to 10%. The geometrically corrected simulations taking into account the retrieved FWHM and the radiometrically corrected measurements match well and enable an improved photometric analysis (Fig. 1).

Acknowledgements

We thank the following institutions and agencies for support of this work: Italian Space Agency (ASI, Italy). Centre National d'Etudes Spatiales (CNES, France), DLR (Germany). D.K. acknowledges DFG-grant KA 3757/2-1.

References

[1] Ciarniello M. et al., 2015, Astron. Astrophys., 583, A31; [2] Coradini A. et al., 2007, Space Sci. Rev., 128(1), 529-559; [3] Hapke B., 2012, Theory of Reflectance and Emittance Spectroscopy, 2nd Ed., Cambridge Univ. Press; [4] Shkuratov Y. et al., 2011, Planet. Space Sci. 59(13), 1326-1371; [5] Filacchione G., 2006, PhD thesis; [6] Raponi A. et al., 2019, submitted to Science; [7] Acton C.H., 1996, Planet. Space Sci., 44(1), 65-70; [8] Preusker F. et al., 2017, Astron. Astrophys., 607, L1; [9] Brigot G. et al., 2016, IEEE J. Sel. Top. Appl., 9(7), 2923-2939.